SUPPORTING INFORMATION

Mild Synthesis of Cu_2O Nanoparticles Interfaced at the surface of 2D-Al Nanosheets

Manuel Antuch,*[a] Jean François Hochepied,[a,b] Laurent Catoire,[a] Johnny Deschamps*[a]

[a] Unité de Chimie et Procédés (UCP), Ecole Nationale Supérieure de Techniques Avancées (ENSTA), Institut Polytechnique de Paris, 828 Boulevard des Maréchaux, 91120, Palaiseau, France.

[b] MINES ParisTech, PSL Université, Centre des matériaux (CMAT), CNRS UMR 7633, BP 87 91003 Evry, France.

Table of Contents

Experimental details

Reagents

Al (2D nanosheet microstructure) was provided by Toyal Europe and had 50 % of weight composed of a mixture of light aromatic and aliphatic solvent. These 2D-Al nanosheets illustrated Figure S1 were used as received without previous treatment. $Cu(COO)_2 \cdot H_2O$ and diethylenglycol were obtained from Merck. In (> 99.9 %) and Zn (> 99.9 %) were received from Aldrich.

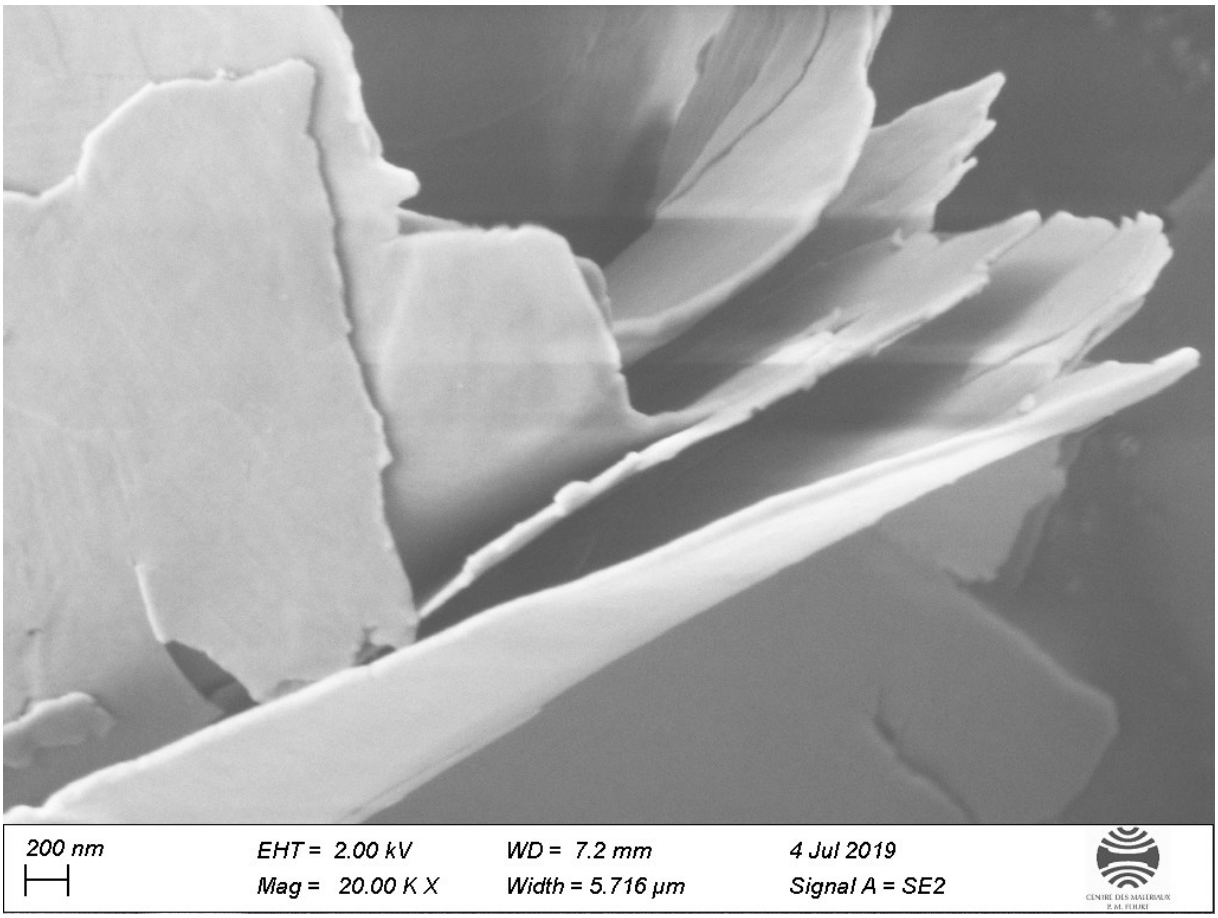

Figure S1. Scanning Electron Microscopy (SEM) image of the unmodified Al nanosheets.

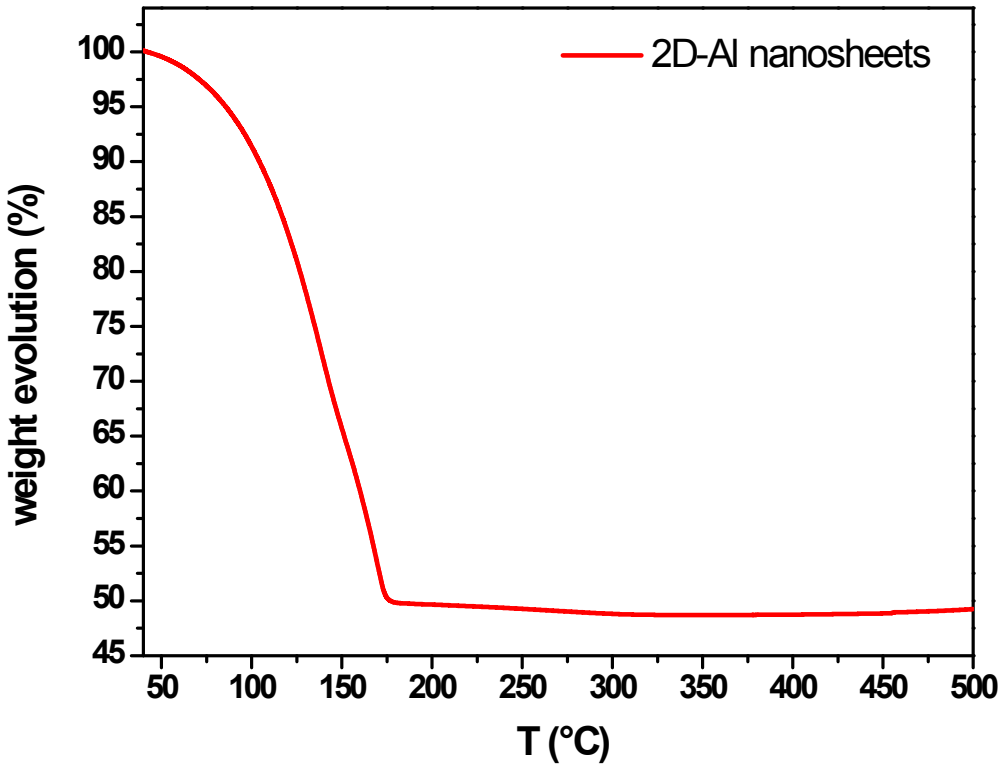

Figure S2. TGA curve for the Al (2D nanosheet microstructure) as obtained from TOYAL Europe. Note that 50 % of the weight corresponds to volatile components.

Apparatus

X-ray diffractograms were acquired in a Bruker D8 diffractometer using Co $K_{\alpha 1}$ radiation, λ = 1.789˚A and a scintillation counter.

Scanning electron microscopy (SEM) images were obtained at 2-3 kV on a Zeiss Sigma 300 microscope using a secondary electron (SE) detector. Elemental microanalyses were carried out in this SEM equipped with a Bruker Quantax 6030 energy dispersive spectrometer (EDS) at 10 kV for an acquisition of 500 kcounts per scan.

X-ray Photoelectron Spectroscopy was recorded in a Thermo Fisher Scientific equipment (base pressure of 10^{-9} mbar). The spectrometer had a monochromatic Al source (Al K_{α}, 1486.7 eV). The analyzer was operated at 0° take off. A pass energy of 50 eV and a step of 0.1 eV was employed for the acquisition of narrow windows.

Thermal analyses were investigated by using Setaram LabSys evo TGA-DTA system. Gas flow (either air or N_2) was set to 30 mL.s^{-1}. The temperature range for the analysis was between 40 °C and 925 °C. Heating rates of 10 °C.min^{-1} and 20 ° C.min^{-1} were employed.

X-ray photoelectron spectroscopy (XPS) characterization was carried out with a Thermo Fisher Scientific instrument; base pressure below 10^{-9} mbar. A monochromatic aluminum source (Al Ka,1486.7 eV) was employed with a spot size of 400 mm and an irradiated area of 1 mm^2.

Synthesis

As a general procedure, 2.47 g of Al (corresponding to 2.47/2 = 1.235 g of Al; 45.8 mmol) were mixed with 10.51 g of copper acetate ($Cu(CH_3COO)_2 \cdot H_2O$) (52.6 mmol) and subsequently 100 mL of diethyleneglycol were added to a Teflon vessel. A magnetic bar for stirring was introduced in the vessel at this stage. The mixture was then put in an ultrasonic bath for 30 minutes until the full dispersion of the Al nanoflakes and the dissolution of $Cu(CH_3COO)_2 \cdot H_2O$. Subsequently, the Teflon vessel was put in a stainless steel autoclave. The autoclave was placed on top of a magnetic stirrer, and it was heated via a heating blanket. Heating was performed from room temperature (20 °C) till 130 °C in 1h, the temperature was then kept at 130 °C for three additional hours. Then the heating blanket was disconnected and the autoclave was cooled down to room temperature with a water bath. The cooling time was 30 minutes. The final product was filtered over Whatman paper with the aid of a vacuum pump. The product was washed 5 times with methanol and subsequently 5 times with water in order to remove the excess of solvent from the synthesis. The final product was dried overnight in an oven at 40 °C and 3.2 g of a grey powder is obtained (Figure S3-a).

Additional comments on the reaction conditions

Heating till a temperature of 310 °C instead of 130 °C for 1h yielded the reduction of Cu(II) to Cu(0) and the dissolution of Al. The XRD pattern of the solid obtained under these conditions is depicted in Figure S3, where the reflections of Cu(0) are the only observed (Figure S3-b).

To purify the final product (Al/Cu_2O nanothermite), filtration is the best manner to proceed due to its simplicity and effectivity. As an alternative, the product may be centrifugated at

3800 rpm for 15 minutes and easily recovered. However, thorough washing is essential because traces of diethyleneglycol cause the subsequent reduction of Cu_2O to Cu. Such reduction is readily observed with bare eye, since the final product just after reaction is grey, but the next day is reddish. This evidently spoiled the nanothermite (Figure S3-c) given the coexistence of Al, Cu_2O and Cu.

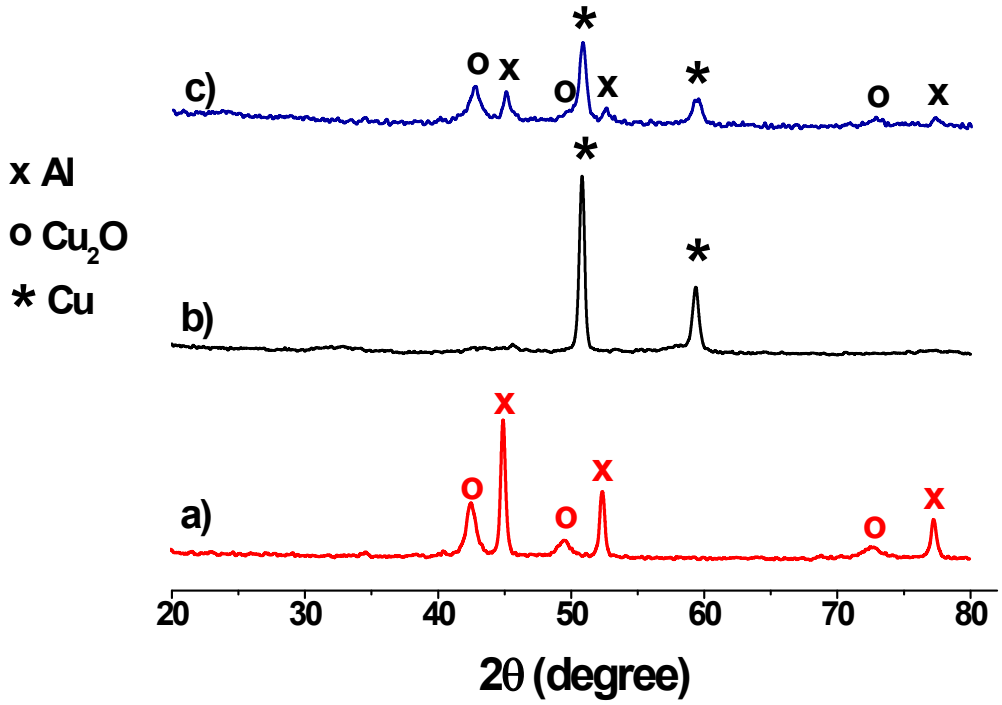

Figure S3. XRD pattern of different products of reaction depending on the conditions, as described in the main text. Note that the diffractogram of item (a) is identical to that presented in Figure S4-a (red) and Figure 2-e (pristine) in the main manuscript. It was included in different figures for the sake of simplicity in the comparison with other diffractograms.

Safety considerations

The Al/Cu_2O nanothermite reported in this work could be handled for several months in laboratory conditions as any other normal solid. Nevertheless, all handling of the Al/ Cu_2O nanothermite was carried out using a laboratory helmet. During this time, no indications of self-ignition or sparks were noticed. The material has a low sensitivity, as reflected in Figure S4 and Figure S5. Nevertheless, this may be a hazardous compound that must be treated with extreme care in order to avoid accidents caused by undesired reaction.

In order to dispose this nanothermite, it is advisable to treat it with a concentrated base (NaOH or KOH), in order to dissolve the Al, and therefore neutralize the compound. This procedure should also be performed with all glassware, Whatman filter paper and the autoclave that were in contact with the nanothermite. It is worth noting that the dissolution process of Al with concentrated base is accociated to a hydrogen clearing. The mixture of hydrogen and a nanothermite may be dangerous, and this procedure needs to be performed with extreme care and adequate mechanical protection. In our experience, the traces of Al/Cu_2O nanothermite from the autoclave and the Whatman paper could be treated with NaOH and rough reactions were observed.

Regarding the risks for health, Al does not present danger for acute poisoning, though, it has pernicious effects for the immune system.[1,2] On the other hand, Cu is present in important metalloenzymes in the body. Though, its presence as a free ion in the human organism may cause oxidative stress.[3] We recommend that this nanothermite should be handled with gloves. Moreover, we recommend avoiding contact with mucosae and not to inhale the product.

Stability

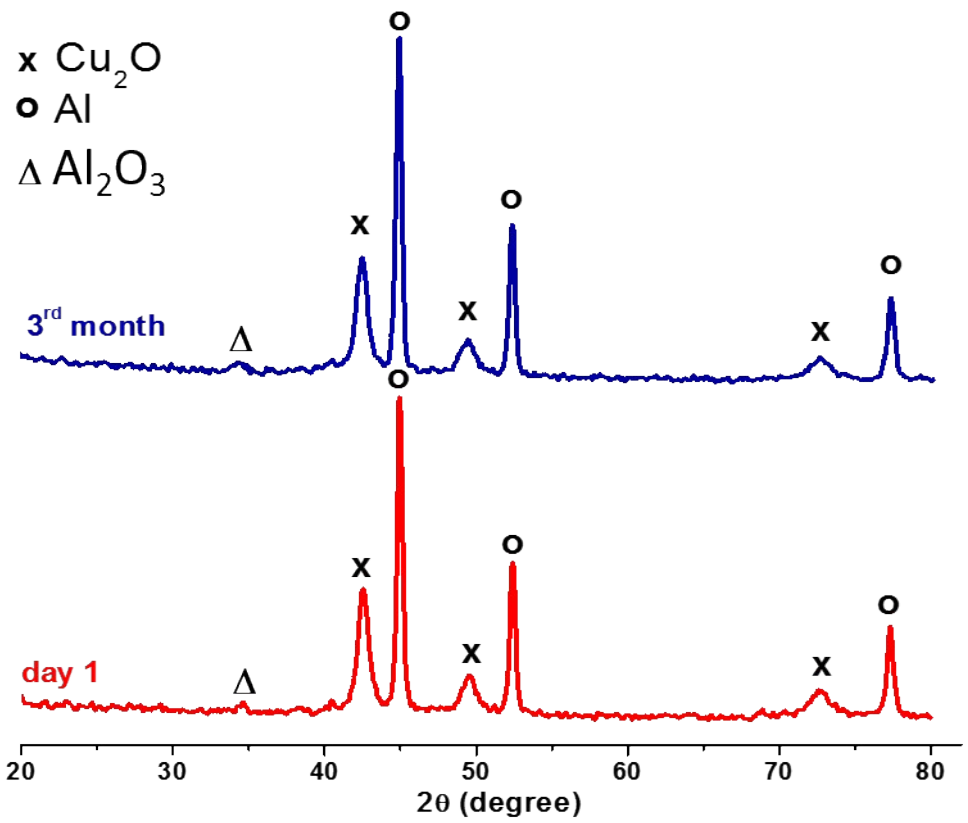

Figure S4. a) XRD pattern of the Al/Cu_2O nanothermite just after synthesized and three months after.

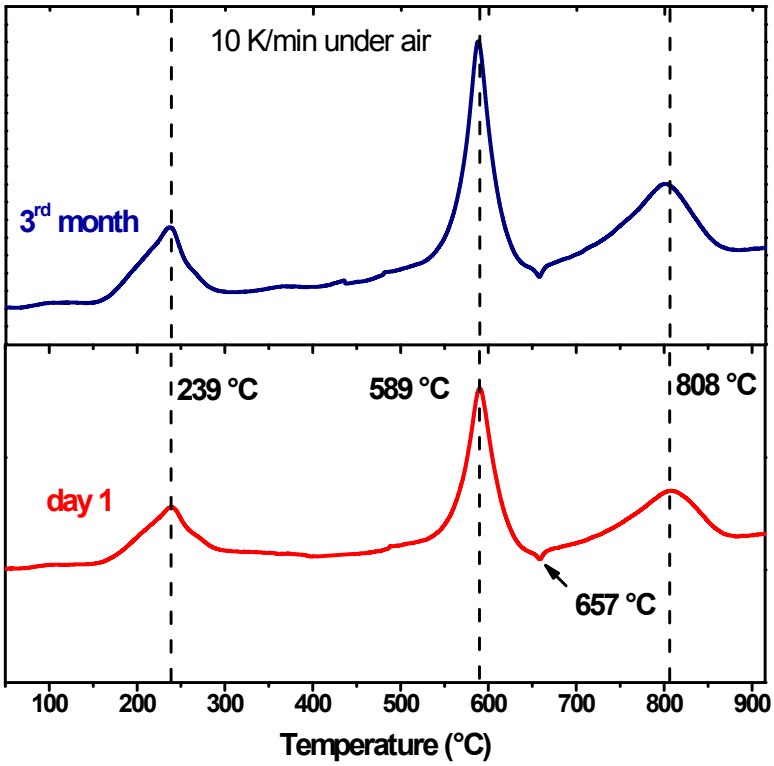

Figure S5. DTA curve of the Al/Cu_2O nanothermite just after synthesized and three months after.

Microstructure after reaction

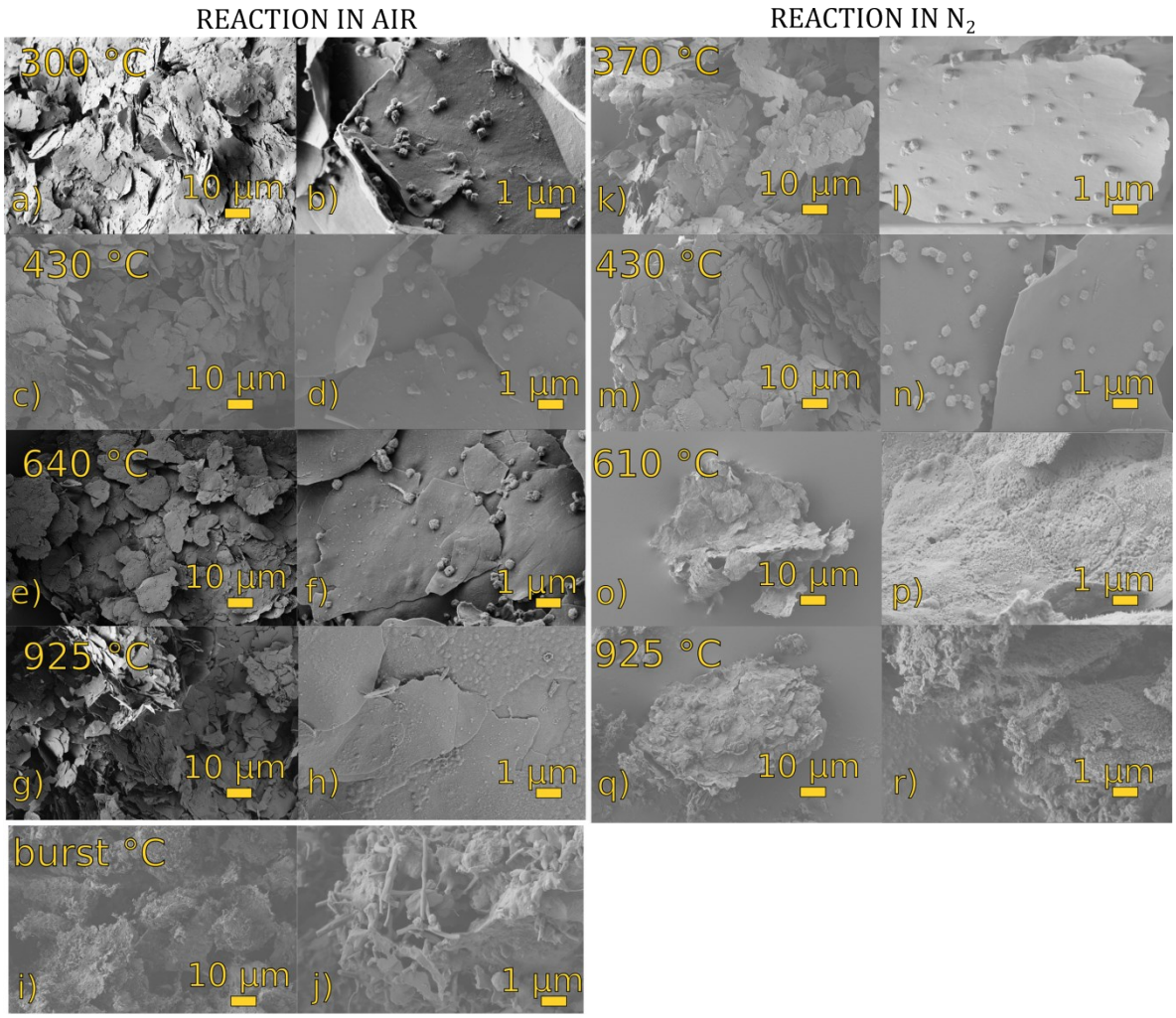

Figure S6. SEM micrographs of the reaction progress under different conditions. Items (a) and (b) correspond to a different magnification of the sample; likewise for the pairs (c) and (d); (e) and (f); (g) and (h); (i) and (j); (k) and (k); (m) and (n); (o) and (p); (q) and (r).

Elemental cartography after reaction

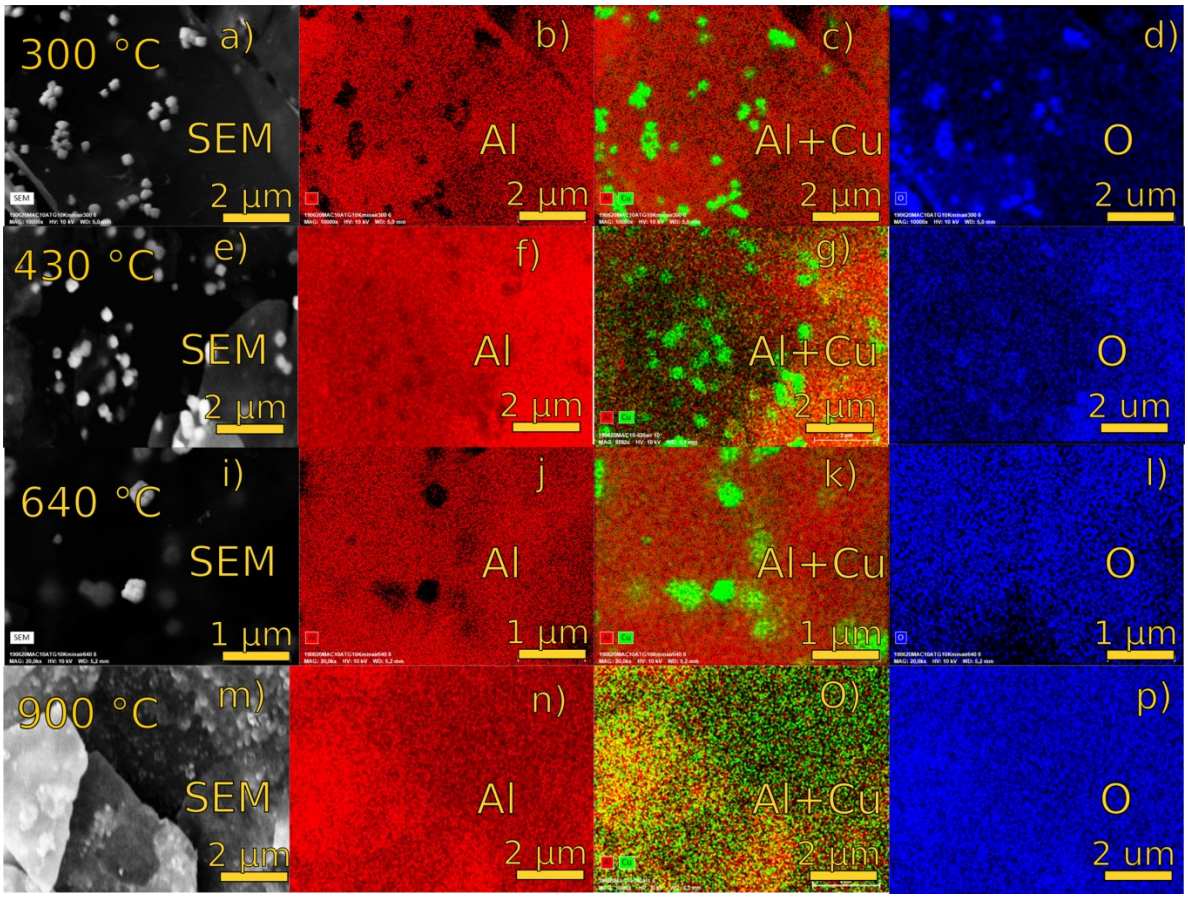

Figure S7. EDS cartographies of the reaction progress under air atmosphere till different heating temperatures.

XPS characterization

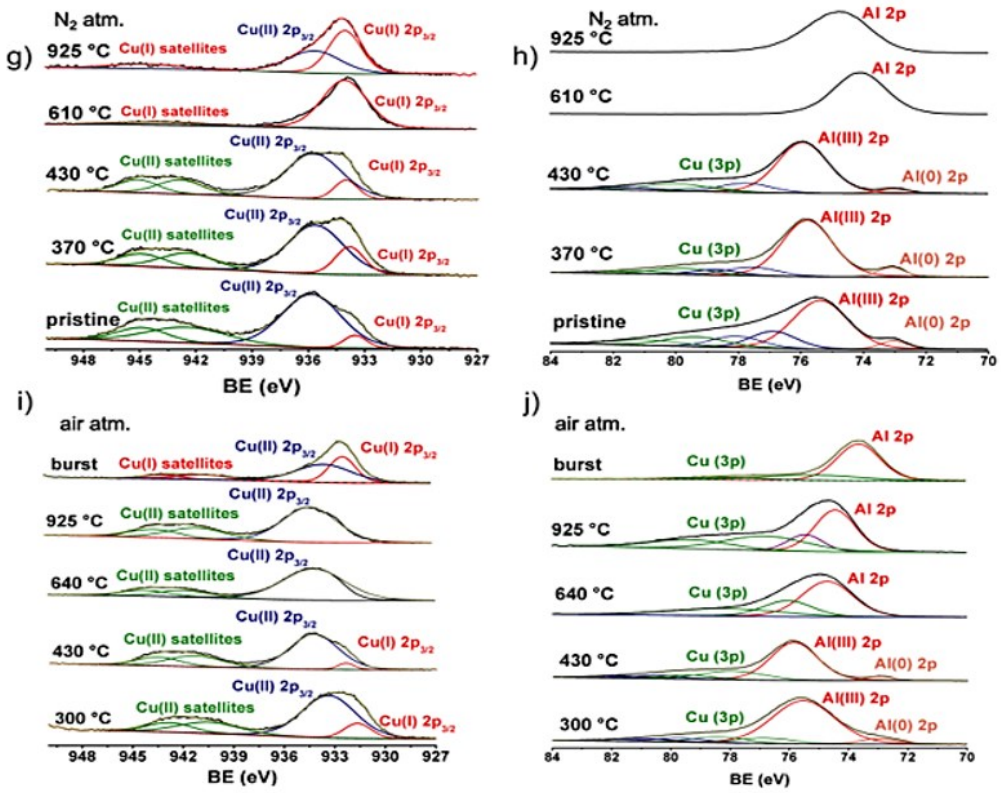

Figure S8. g) XPS spectrum of the Cu 2p3/2 and h) Al 2p core levels for the different products obtained after reaction under N2 atmosphere; i) XPS spectrum of the Cu 2p3/2 and j) Al 2p core levels for the different products obtained after reaction under air.

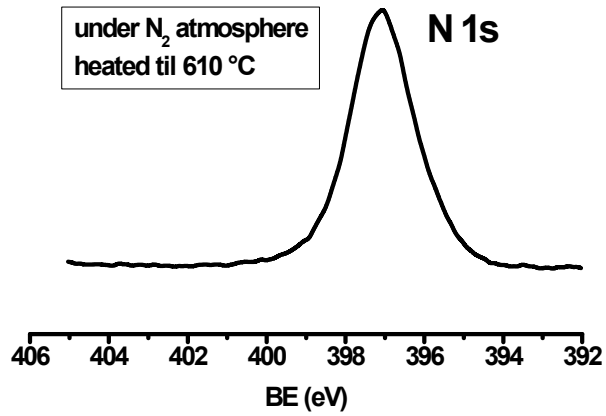

Figure S9. XPS N1s spectrum of the product of Al/Cu_2O combustion after heating at 610 °C under N_2 atmosphere.

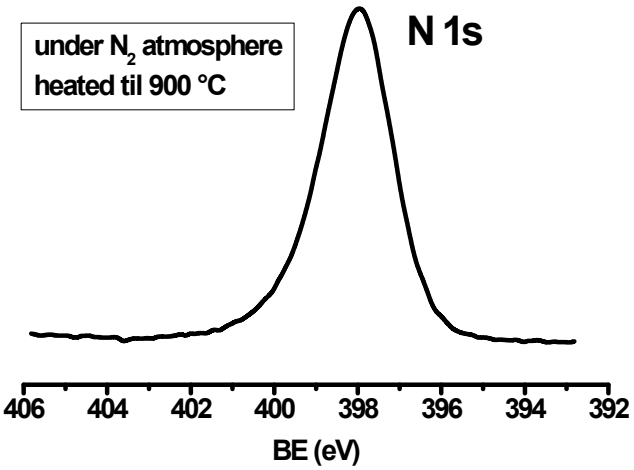

Figure S10. XPS N1s spectrum of the product of Al/Cu_2O combustion after heating at 900 °C under N_2 atmosphere.

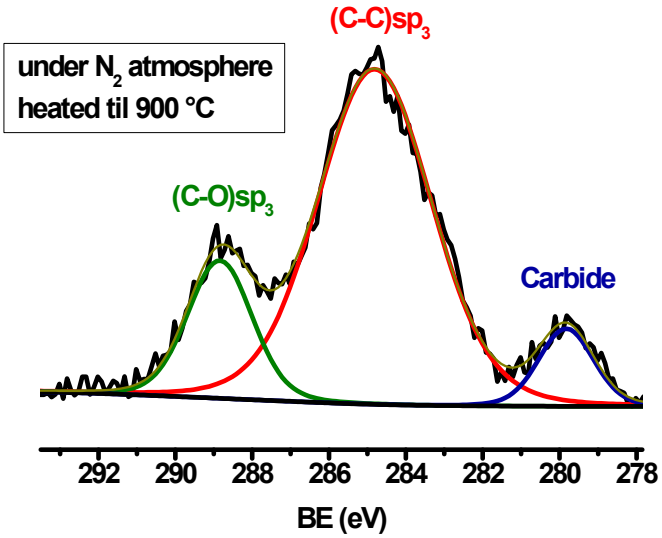

Figure S11. XPS C1s spectrum of the product of Al/Cu_2O combustion after heating at 900 °C under N_2 atmosphere. The formation of the carbide suggests that small amounts of diethyleneglycol remained strongly adsorbed at the surface even after heating till 925 °C. Metallic carbides have been reported since long;[4] Cu may react with C in small amounts, while Al forms the stoichiometric compound Al_4C_3. The XPS evidence does not allow concluding whether this is copper or aluminum carbide.

Table S1. Tabulation of heat released by different nanothermites

System Characteristics		Temperature (°C)	Heat released ($J.g^{-1}$)	Year	Reference
Al/CuO (calculated)		25	4075.2	1998	5
Al/Cu_2O (calculated)		25	2405.8		
Magnetron Sputtered Al–Cu_2O Multilayers	0 nm of Cu	50 –725	1208 ± 262	2017	6
	25 nm of Cu		1135 ± 126		
	50 nm of Cu		951 ± 111		
	75 nm of Cu		651 ± 30		
	100 nm of Cu		595 ± 16		
3D Ordered Macroporous Structured Fe_2O_3/Al Nanothermite Film		480 – 638	902	2013	7
		735 – 813	1929		
Nano-Al/NiO Thermite Film by Electrophoretic Deposition	Fuel to Oxidizer ratio of 1.90	550 – 600	601	2015	8
	Fuel to Oxidizer ratio of 1.23	550 – 600	931		
	Fuel to Oxidizer ratio of 0.63	550 – 600	688		
Nanothermite colloids mechanically mixed with TNT	TNT (reference)	292	520	2019	9
	Al/TNT	255	925		
	(CuO/Al)/TNT CuO particles of 15 nm	242	1213		
Electrochemical synthesis of Al/CuO thermite films	CuO-NPs/Al-NPs	200 – 300	0	2019	10
		550 – 700	904 ± 50		
		Total	904 ± 50		
	Al/CuO (5 min deposition)	200 – 300	191 ± 10		
		550 – 700	1178 ± 50		
		Total	1369 ± 60		
	Al/CuO (10 min deposition)	200 – 300	233 ± 15		
		550 – 700	1776 ± 40		
		Total	2009 ± 55		
	Al/CuO (15 min deposition)	200 – 300	225 ± 5		
		550 – 700	1311 ± 60		
		Total	1536 ± 65		
Al-CuO nanothermites with addition of multilayer graphene	0 %	596 – 677	1591.5 ± 26.2	2018	11
	1 %	596 – 711	1679.0 ± 22.6		
	2 %	596 – 706	1652.5 ± 31.8		
	3 %	595 – 704	1530.0 ± 42.4		
	5 %	595 – 698	1489.5 ±		

			57.3		
	10 %	595 − 684	1465.0 ± 49.5		
Al/CuO Nanothermites with Ammonium Perchlorate as additive	NH_4ClO_4 7.5%	510 − 570[a]	828.8	2018	12
		640 − 795[a]	287.2		
		Total	1113.0		
	NH_4ClO_4 5.0%	510 − 570[a]	795.4		
		640 − 795[a]	308.7		
		Total	1104.1		
	NH_4ClO_4 2.5%	510 − 570[a]	601.5		
		640 − 795[a]	335.1		
		Total	936.6		
	NH_4ClO_4 0.0%	510 − 570[a]	792.1		
		640 − 795[a]	0		
		Total	792.1		
Salix Leaf-like CuO and Nano-Al through Electrophoretic Deposition		Around 590	706.5	2016	13
		Around 660	748.1		
		Total	1454.6		
CuO nanowires and nanopowders coated with Al	CuO nanowires coated with deposited nano-Al	Around 600	1186	2011	14
	CuO nanopowder coated with deposited nano-Al	Around 539	962.9		

[a]Estimated from Figure 5 of the original paper.

Heat release calibration

The calibration of the heat released was performed by using two different standards, namely, (Indium) In and (Zinc) Zn. Different masses of both substances were put in the DTA analyzer and the temperature was swept till the full melting.

The area under the curves (after blank correction) was used as a measure of the heat evolved during fusion at constant pressure (Figure S11). The enthalpy of fusion for In was set to 3291 J/mol,[15] while that of Zn was set to 7070 J/mol.[16] The heat values reported in Table S2 were found by using both Zn and In standards, and both values were essentially the same, within experimental uncertainty.

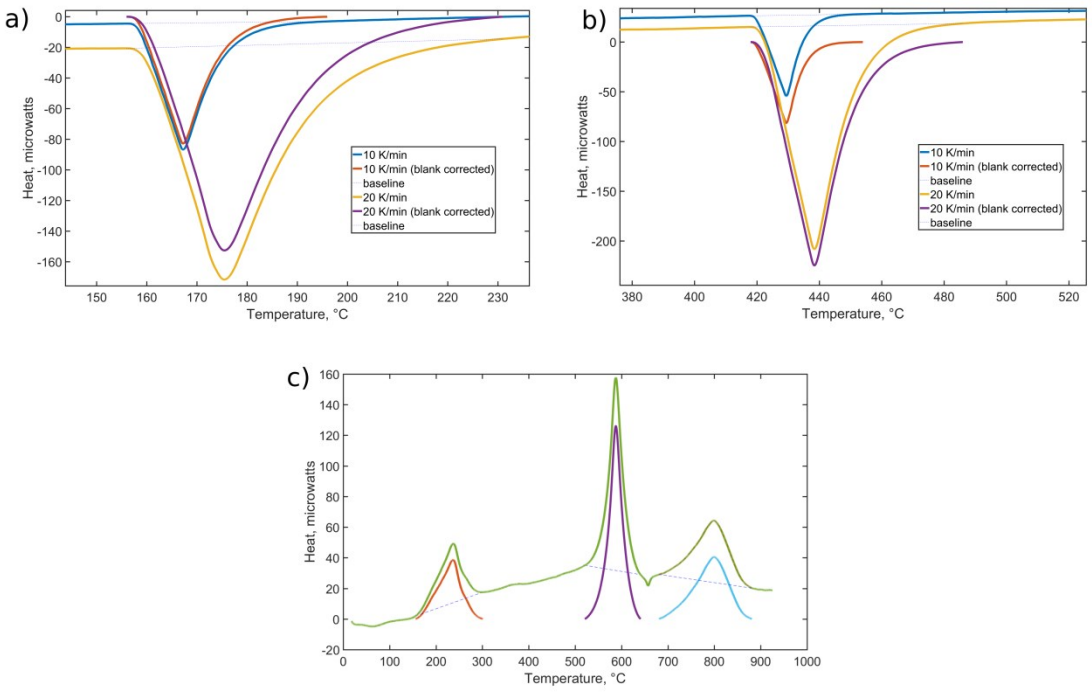

Figure S12. Typical DTA curves for a) In and b) Zn samples; c) determination of the area under the DTA curve for the three thermal processes occurring in the Al/Cu_2O nanothermite.

Table S2. Tabulation of the heat released by the nanothermite obtained in this work*

Atmosphere	Temperature range (°C)	Heat released (Jg^{-1})
Air	150 − 300	1357 ± 148
	520 − 640	3313 ± 228
	700 − 900	2171 ± 19
	total	6841 ± 272
N_2	160 − 320	1328 ± 27
	520 − 640	1618 ± 305
	total	2946 ± 306

*errors were determined from four independent measurements.

References

1 C. Exley. The Toxicity of Aluminium in Humans. *Morphologie*, 2016, **100** (329), 51–55.

2 M. Comet, C. Martin, F. Schnell, D. Spitzer, Nanothermites: A Short Review. Factsheet for Experimenters, Present and Future Challenges. *Propellants, Explos. Pyrotech.*, 2019, **44** (1), 18–36. https://doi.org/10.1002/prep.201800095.

3 L. M. Gaetke and C. K. Chow, Copper Toxicity, Oxidative Stress, and Antioxidant Nutrients. *Toxicology*, 2003, **189** (1–2), 147–163. https://doi.org/10.1016/S0300-483X(03)00159-8.

4 G.N.H. Metallic Carbides. *Nature*, 1896, **54**, 357.

5 S. Fischer, M. Grubelich, Theoretical Energy Release of Thermites, Intermetallics, and Combustible Metals. *24th Int. Pyrotech. Semin.*, 1998, **220** (3), 56. https://doi.org/10.2172/658208.

6 A. H. Kinsey, K. Slusarski, S. Sosa, T. P. Weihs, Gas Suppression via Copper Interlayers in Magnetron Sputtered Al-Cu2O Multilayers. *ACS Appl. Mater. Interfaces*, 2017, **9** (26), 22026–22036. https://doi.org/10.1021/acsami.7b03071.

7 W. Zhang, B. Yin, R. Shen, J. Ye, J. A. Thomas, Y. Chao, Significantly Enhanced Energy Output from 3D Ordered Macroporous Structured Fe2O3/Al Nanothermite Film. *ACS Appl. Mater. Interfaces*, 2013, **5** (2), 239–242. https://doi.org/10.1021/am302815y.

8 D. Zhang and X. Li, Fabrication and Kinetics Study of Nano-Al/NiO Thermite Film by Electrophoretic Deposition. *J. Phys. Chem. A*, 2015, **119** (20), 4688–4694. https://doi.org/10.1021/jp5129113.

9 M. G. Zaky, A. M. Abdalla, R. P. Sahu, I. K. Puri, M. Radwan, S. Elbasuney, Nanothermite Colloids: A New Prospective for Enhanced Performance. *Def. Technol.*, 2019, **15** (3), 319–325. https://doi.org/10.1016/j.dt.2018.08.016.

10 B. Hu, W. Zhang, C. Yu, Z. Zheng, Y. Chen, J. Wang, J. Liu, K. Ma, W. Ren, Electrochemical Synthesis of Al/CuO Thermite Films on Copper Substrates. *Ind. Eng. Chem. Res.*, 2019, **58** (17), 7131–7138. https://doi.org/10.1021/acs.iecr.8b05959.

11 J. Shen, Z. Qiao, J. Wang, G. Yang, J. Chen, Z. Li, X. Liao, H. Wang, M. R. Zachariah, Reaction Mechanism of Al-CuO Nanothermites with Addition of Multilayer Graphene. *Thermochim. Acta*, 2018, ***666*** (June), 60–65. https://doi.org/10.1016/j.tca.2018.06.005.

12 J. Dai, F. Wang, C. Ru, J. Xu, C. Wang, W. Zhang, Y. Ye, R. Shen, Ammonium Perchlorate as an Effective Additive for Enhancing the Combustion and Propulsion Performance of Al/CuO Nanothermites. *J. Phys. Chem. C*, 2018, **122** (18), 10240–10247. https://doi.org/10.1021/acs.jpcc.8b01514.

13 Y. Yin and X. Li, Building Energetic Material from Novel Salix Leaf-like CuO and Nano-Al through Electrophoretic Deposition. *Bull. Korean Chem. Soc.*, 2016, **37** (11), 1827–1830. https://doi.org/10.1002/bkcs.10983.

14 D. K. Kim, J. H. Bae, M. K. Kang, H. J. Kim, Analysis on Thermite Reactions of CuO Nanowires and Nanopowders Coated with Al. *Curr. Appl. Phys.*, 2011, **11** (4), 1067–1070. https://doi.org/10.1016/j.cap.2011.01.043.

15 D. G. Archer and S. Rudtsch, Enthalpy of Fusion of Indium: A Certified Reference Material for Differential Scanning Calorimetry. *J. Chem. Eng. Data*, 2003, **48** (5), 1157–1163.

16 F. Grønvold and S. Stølen, Heat Capacity of Solid Zinc from 298.15 to 692.68 K and of Liquid Zinc from 692.68 to 940 K: Thermodynamic Function Values. *Thermochim. Acta*, 2003, **395** (1–2), 127–131. https://doi.org/10.1016/S0040-6031(02)00217-4.